Sensors & Transducers, Vol. 181, Issue 10, October 2014, pp. 219-226

Sensors & Transducers

A Coupled Model for Work Roll Thermal Contour with Subsectional Cooling in Aluminum Strip Cold Rolling

[1] Shao Jian, [1] He Anrui, [1] Jiang Li, [1] Yao Chihuan, [2] Xu Lei
[1] National Engineering Research Center for Advanced Rolling Technology, University of Science and Technology Beijing, Beijing, 100083, China
[2] Guangxi Liuzhou Yinhai Aluminum Co., Ltd., Liuzhou, 545006, China
[1] Tel.:+86 01062332598
E-mail:ustbshao@163.com

Received: 30 July 2014 /Accepted: 30 September 2014 /Published: 31 October 2014

Abstract: Little attention had been given to the evaluation of subsectional cooling control ability under complicated working conditions. In this paper, heat generation was calculated by using finite difference method. Strip hardening, work roll elastic deformation and elastic recovery of strip were taken into account. The mean coefficient of convective heat transfer on work roll surface was simulated by FLUENT. Calculation model had used the alternative finite difference scheme, which improved the model stability and computing speed. The simulation result shows that subsectional cooling control ability is different between different rolling passes. Positive and negative control abilities are roughly the same in the same pass. The increase of rolled length, working pressure of header and friction coefficient has positive effect on subsectional cooling control ability, and the rolling speed is on the contrary. On the beginning of the pass, when work roll surface has not reached the stable temperature, control ability of subsectional cooling is mainly affected by rolled length. The effect of mean coefficient of convective heat transfer and coefficient of friction is linear. When rolling speed is over 500 m/min, control ability of subsectional cooling becomes stable. *Copyright © 2014 IFSA Publishing, S. L.*

Keywords: Aluminum, Cold rolling, Subsectional cooling, Thermal expansion, Alternative finite difference.

1. Introduction

Subsectional cooling is widely used in cold rolling, and flatness control effect is strongly related to the thickness of strip. According to research, 90 % of flatness is controlled by subsectional cooling in foil rolling [1]. With the application of new type high efficient nozzle in mills cooling system, subsectional cooling is more and more widely used and gradually plays an important role in common specifications nonferrous metal rolling. Currently, four high single stand mill is the mainstream configuration in aluminum cold rolling. In cold rolling, flatness is controlled by hydraulic work roll bending, work roll leveling and subsectional cooling, and subsectional cooling is the only mean to control high order and local flatness of strip.

Many studies have been conducted for flatness control using subsectional cooling in cold rolling, and much of them are concentrated in modern advanced control field, with no mechanism model supported, such as fuzzy control, neural network control [2-5], etc. In cold rolling, temperature difference between work roll and strip is much smaller than hot rolling, resulted that the thermal behavior of work roll and strip is strongly coupled. Work roll thermal expansion is directly controlled by subsectional cooling. On the other hand, work roll thermal load is

affected by rolling speed, cooling intensity, work roll temperature and other rolling parameters, and these rolling parameters are nonlinearly coupled. As a consequence, little attention had been given to the evaluation of subsectional cooling control ability under complicated working conditions.

Based on the subsectional cooling system of 1850mm aluminum cold rolling mill, the main objective of this paper is to predict the subsectional cooling control ability by considering work roll spray cooling, deformation heat generation, heat transfer between work roll and strip.

2. Configuration of Subsectional Cooling

Work roll cooling medium is kerosene. In order to reduce the residue of kerosene on the strip and improve the efficiency of air spray on the export side of mill, work roll cooling equipment is installed only on the entry side of the mill. As shown in Fig. 1, each work roll has two rows of spray nozzles. 34 nozzles have been configured in each row, with the spacing of 52 mm and 52 degrees tilt angle. These nozzles have flow of 31.6 L/min under nominal pressure (5 bar). In addition, the nozzles just have on and off two type mode.

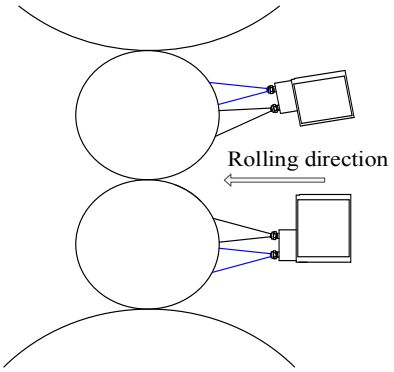

Fig. 1. Configuration of subsectional cooling system.

3. Mathematical Model of Work Roll Thermal Contour

3.1. Equation of Heat Conduction

The coolant flow is unevenly sprayed on work roll in both axial and circumferential direction, which leads to uneven temperature distribution of work roll. Many studies have shown that uneven temperature distribution of work roll in circumferential direction occurs only in a very thin layer over the roll surface, and big temperature gradient is limited at the bite region. Therefore, in cold rolling heat conduction along the circumferential direction of work roll can be ignored. Work roll heat conduction can be written as follow [6, 7].

$$\rho c_p \frac{\partial T_r}{\partial t} = k_r \left(\frac{\partial^2 T_r}{\partial y^2} + \frac{1}{r} \cdot \frac{\partial T_r}{\partial r} + \frac{\partial^2 T_r}{\partial r^2} \right), \quad (1)$$

where T_r is the temperature of work roll, ρ is the density of work roll, c_p is the specific heat capacity of work roll, k_r is the thermal conductivity of the work roll, r is radial coordinate, y is axial coordinate.

Fig. 2 shows the heat transfer boundary of work roll along the circumferential direction. Work roll rotates at a speed of ω, different temperature calculation planes along the circumferential direction of work roll are represented by k, k+1$\cdots$$k$+i. d$\theta_i$ is the angle difference between plane k+i and k+i+1. dt_i equals dθ_i divided by ω. As a consequence, plane k+i will rotate to position of plane k+i+1 after dt_i, and temperature distribution integrated by dt_i on plane k+i can represent the changes on plane k+i when it rotates dθ_i degrees. The temperature distribution calculations on different planes are independent between each other because of the heat conduction along the circumferential direction of work roll is ignored. If the boundary conditions of plane k+i and k+i+1 are same, temperature distribution on plane k+i at the time of t+dt_i is same as k+i+1 at the time of t. From the above analysis can be introduced that the calculation of temperature distribution of whole work roll can be simplified to just calculating the temperature distribution on plane k+i which rotates a round.

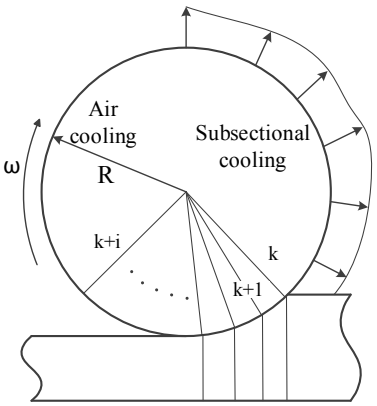

Fig. 2. Heat transfer boundary of work roll along the circumferential direction.

Similar to work roll, heat conduction along the rolling direction of strip is ignored, and heat conduction of strip is shown as follow:

$$\rho_s c_{ps} \frac{\partial T_s}{\partial t} = k_s \left(\frac{\partial^2 T_s}{\partial y^2} + \frac{\partial^2 T_s}{\partial z^2} \right) + q_d, \quad (2)$$

where T_s is the temperature of strip, ρ_s is the density of strip, c_{ps} is the specific heat capacity of strip, k_s is the thermal conductivity of strip, q_d is the deformation heat flux of strip, z is coordinate along the thickness direction of strip.

3.2. Friction Heat and Deformation Heat

In bite region, the heat generated by strip plastic deformation and friction between work roll and strip is the main source of the temperature rise in cold rolling, and the amount is determined by rolling force, friction stress and relative slipping speed, affected by hardening of material, friction condition, plastic recovery of strip, plastic deformation of work roll, rolling tension, reduction rate, thickness of strip, etc.

The widely used slab method is used to analysis the rolling force in cold rolling. The Karman balance equation is shown as follow:

$$d\sigma_x + \left(\sigma_x + p_y\right)\frac{dh}{h} \pm \frac{2\tau_x dx}{h} = 0, \tag{3}$$

where σ_x is the stress along rolling direction, p_y is the rolling force, h is the thickness of strip, τ_x is the horizontal friction stress.

For friction model, full sticking model is traditionally used and preparatory displacement model is more reliable for friction behavior near the neutral point zone of bite region [8]. In this paper, all of these friction models have been combined and the expression is shown as follows:

$$\tau = \begin{cases} \mu p_y & \left(p \le \sigma_s\right) \\ \sigma_s & \left(p \ge \sigma_s\right) \\ \dfrac{\left(x_n - x\right)\mu p'}{l_n/2} & \left(x_n - l_n/2 \le x < x_n\right) \\ \dfrac{\left(x - x_n\right)\mu p''}{l_n/2} & \left(x_n \le x \le x_n + l_n/2\right) \end{cases}, \tag{4}$$

$$l_n = \frac{2fp_m/\sigma_m}{0.75 - \left(fp_m/\sigma_m\right)^2} h_m, \tag{5}$$

where μ is the friction coefficient, σ_s is the shear strength, l_n is the width of sticking zone at neutral point, p' is the rolling force between backward slip zone and sticking zone, p'' is the rolling force between forward slip zone and sticking zone. p_m is the average rolling force, h_m is the thickness of strip at neutral point, σ_m is the yield stress of strip, f is the friction factor related to friction coefficient and bite angle.

The elastically compressed radius of work roll is calculated by Hitchcock formulation [9]:

$$R' = R\left[1 + \frac{2}{\Delta h}\frac{8\left(1-\nu^2\right)}{\pi E}p\right], \tag{6}$$

where E is the modulus of elasticity of work roll, v is the passion ratio of work roll, Δh is the reduction of thickness, p is the unit width rolling force, R is the original radius of work roll.

Deformation heat q_d is obtained by following expression:

$$q_d = p_y \ln\left(\frac{dh}{h}\right) h_{exit} V_{exit}, \tag{7}$$

where h_{exit} is the thickness of strip at exit side, V_{exit} is the exit speed of strip.

Frictional heat q_f can be calculated by friction stress and related slipping speed, expression is given as follows:

$$q_f = \tau \Delta l \left|V_{slip}\right|, \tag{8}$$

where Δl is the length of contact arc.

3.3. Boundary Condition of Heat Transfer

Work roll is surrounded by different types of thermal boundary condition, including heat transfer between work roll and strip, work roll and air, work roll and coolant medium and etc.

1) Heat transfer between work roll and strip

Thermal contact conductance model is more reliable in cold rolling, which has taken rolling force, surface roughness, thermal conductivity, and hardness into consideration, which can be expressed as follows [10, 11]:

$$-k_r\left(\partial T_r/\partial n\right)_b = h_c\left(T_r|_b - T_s|_b\right) - q_f/2, \tag{9}$$

$$-k_s\left(\partial T_s/\partial n\right)_b = h_c\left(T_s|_b - T_r|_b\right) - q_f/2, \tag{10}$$

where k_r is the thermal conductivity of work roll, k_s is the thermal conductivity of strip, h_c is the thermal contact conductance between work roll and strip, $T_r|_b$ is the surface temperature of work roll, $T_s|_b$ is the surface temperature of strip.

$$h_c = h_{cs} + h_{cm}, \tag{11}$$

where h_{cs} is the solid contact conductance coefficient, h_{cm} is the lubricant contact conductance coefficient.

$$h_{cs} = 3800 k_h R_a^{-0.257}\left[P/\left(M+P\right)\right]^{0.94}, \tag{12}$$

$$k_h = \frac{2k_s k_r}{k_s + k_r}, \tag{13}$$

$$R_a = \sqrt{R_s^2 + R_r^2}, \tag{14}$$

where k_h is the average thermal conductivity coefficient, M is the hardness of the softer material, P is the average rolling force, R_a is the average surface

roughness, R_s is the surface roughness of strip, R_r is the surface roughness of work roll.

$$h_{cm} = \left(k_m / \delta_m\right) r_{unc}, \tag{15}$$

where k_m is the thermal conductivity of lubricant, δ_m is the average thickness of lubricant, r_{unc} is the non-solid contact ratio of bite region.

2) Heat transfer between work roll and coolant medium.

Heat convection between work roll and coolant medium is main heat dissipation way, which is nonlinearly related with coolant working pressure, distance of the spray headers from the roll, spray angles and spray planes of the nozzle and so on. Equivalent heat convection coefficient is commonly used as bellow:

$$q_{jet} = h_{jet}\left(T_r|_b - T_{jet}\right), \tag{16}$$

where q_{jet} is the heat convection coefficient, h_{jet} is the equivalent heat convection coefficient, T_{jet} is the temperature of lubricant.

Theories and experiments about equivalent heat convection coefficient of spraying cooling during aluminum cold rolling are limited. In this paper, heat convection coefficient of work roll spray cooling is simulated by FLUENT.

Nozzles are periodically installed in axial direction, therefore, only one section of the jet beam is modeled for saving computing time. The temperature of work roll surface is evenly assumed and nozzles are modeled by 10mm×1.5mm rectangles. Physical model and mesh generation are shown in Fig. 3 and boundary condition is shown in Table 1.

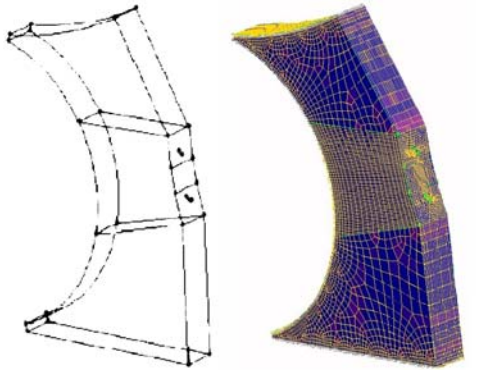

Fig. 3. Physical model and mesh generation by FLUENT.

Table 1. Boundary condition.

Boundary condition	parameters
Inlet pressure	5 bar
Outlet pressure	0 bar
Periodic boundary	Periodic boundary condition
Surface of work roll	323 K, 31.746 rad/s

Equivalent heat convection coefficient simulating result is 4000 W/m^2·K, shown in Fig. 4.

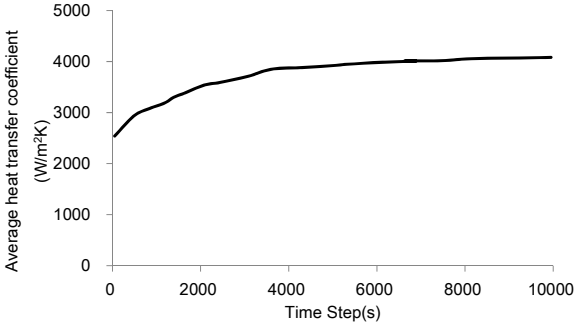

Fig. 4. Equivalent heat convection coefficient of work roll spray cooling.

3) Heat transfer between work roll and air

Heat transfer between work roll and air can be expressed as:

$$h_{air} = 110\frac{\lambda_{air}}{D}\left[\left(0.5\,\mathrm{Re}_w^2 + Gr_D\right)\mathrm{P_r}\right]^{0.35}, \tag{17}$$

where h_{air} is the equivalent heat convection coefficient of air, D is the diameter of work roll, λ_{air} is the thermal conductivity of air, Gr_D is the Graham Akio number, 0~5.4×10^{10}, Re_w is the Reynolds, 0.2×10^6~2.7×10^6 , P_r is the Prandtl number, 0.9.

3.4. Work Roll Thermal Expansion

Subsectional cooling changes cooling intensity of work roll at different position along the axis direction, which brings uneven thermal expansion. The thermal expansion of work roll can be calculated by cylinder thermal expansion formula, shown as follows [12]:

$$u_{x,t} = 4\left(1+\nu\right)\frac{\beta}{R}\int_0^R \left(T_{x,r,t} - T_0\right) r dr, \tag{18}$$

where β is the work roll linear thermal expansion coefficient, R is the work roll radius, $T_{x,r,t}$ is the work roll temperature, T_0 is the work roll original temperature.

4. Mesh Generation and Calculation Step

Mesh is uneven in radius direction and uniform in axis direction. In radius direction, mesh is generated by the ratio of 1.1, and the surface of work roll and strip has the smallest mesh.

In the bite region, temperature rises extremely fast. In order to keep the calculation precision, the time steps in this region area finely divided. On the contrary, time steps in air cooling region and oil

cooling region are properly expanded, saving computing time.

Thermal contact conductance model is applied in this paper, which is generally huge and can easily cause divergence. Smoothing function method is imported to the temperature difference between work roll and strip for improving stability.

$$dT_i^{j+1} = dT_i + b(dT_i^j - dT_i), \quad (19)$$

where dT_{ij} is the temperature difference between work roll and strip at i time step and j iteration step, b is the weight coefficient.

Two dimension alternating difference is used in this model. This method has second order precision and global stability, which is more precise compared with explicit difference method and faster compared with implicit difference method. The program flow chart is shown in Fig. 5.

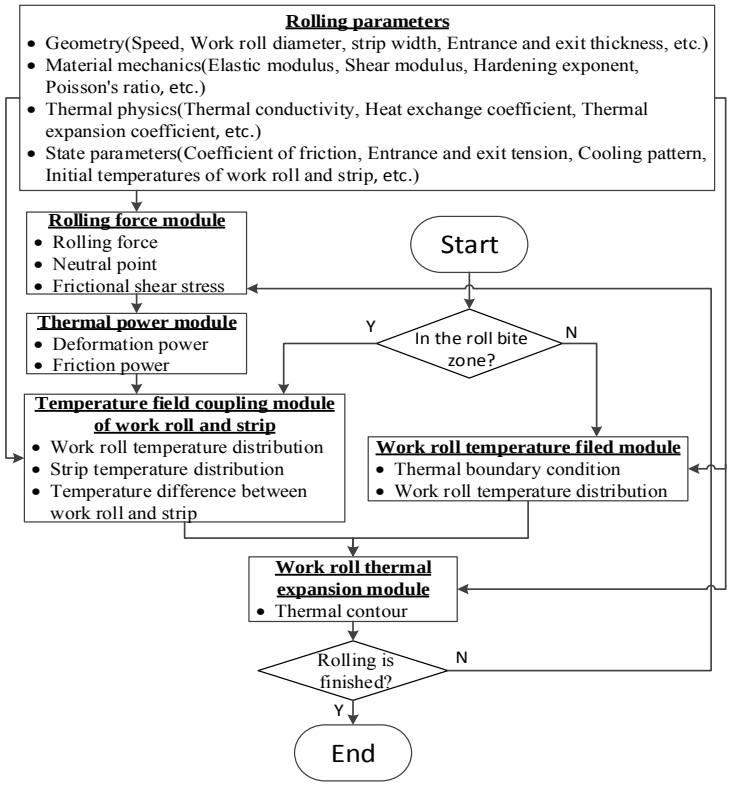

Fig. 5. Program flow chart.

5. Simulation Results of Subsectional Cooling Control Ability

Subsectional cooling control ability is studied at the same rolling length. Based on the actual rolling passes data of alloy 1100 in Table 2, subsectional cooling ability is stimulated, using the coupled heat transfer model of work roll and strip. The simulation conditions are as follows:

1) Set an even level 10 cooling distribution at the first 364 meters rolling length, establishing a steady temperature distribution of work roll surface, and the thermal contour of work roll after this process is referred as the initial thermal contour.

2) Change the duty ratio of each nozzle, when the temperature distribution of work roll surface is steady, setting coolant level as cubic pattern, quartic pattern and local pattern, to achieve the corresponding adjustments to the thermal contour.

3) Calculate the change of thermal contour after 26 m rolling length, analyze the subsectional cooling control ability.

Table 2. Rolling data of alloy 1100.

Pass	1	2	3
Entry thickness/ mm	4.1	2.9	2.2
Exit thickness/ mm	2.9	2.2	1.72
Strip width/ mm	1360	1360	1360
Entry tension/ MPa	9.47	8.68	7.51
Exit tension/ MPa	9.47	8.11	7.25
Work roll diameter/ mm	210.81	210.81	210.81
Rolling speed/ $m \cdot s^{-1}$	4.2	4.7	4.0

5.1. Thermal Contour Adjustment Ranges of Subsectional Cooling

The thermal contour simulation results of alloy 1100 pass 1 is shown in Fig. 6 and Fig. 7. Work roll thermal crown is defined as the diameter difference between the middle and 52 mm to the strip edge. Comparing it with the original thermal contour, the adjustment range of subsectional cooling is obtained. The adjustment range of quartic thermal crown is

-3.62 μm ~ 3.92 μm, which has a positive range slightly larger than the negative. According to the symmetry, the adjustment range of cubic thermal crown is -3.74 μm ~ 3.74 μm.

The thermal contour under local pattern coolant is shown in Fig. 7, cooling and not cooling at certain positions, which from left to right are edge section no. 1, quarter wide section, middle section and edge section no. 2. Except edge section no. 1, the adjustment range of local thermal crown at other sections are almost the same, with a positive and negative range both about 3.78 μm, indicating there is an edge effect of thermal contour only at the edge section no. 1. Due to the larger heat transfer capability at the edge, the nozzles there have a smaller effective width and adjustment range of thermal contour than those at the middle.

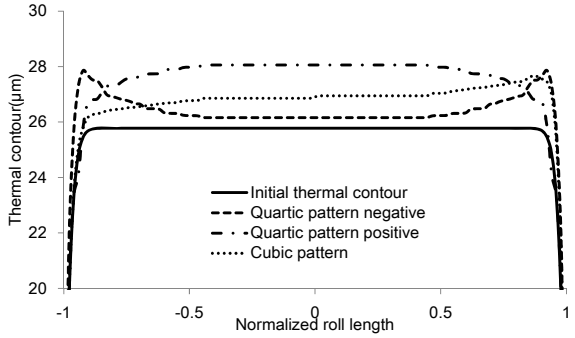

Fig. 6. Thermal contour under cubic pattern and quartic pattern coolant.

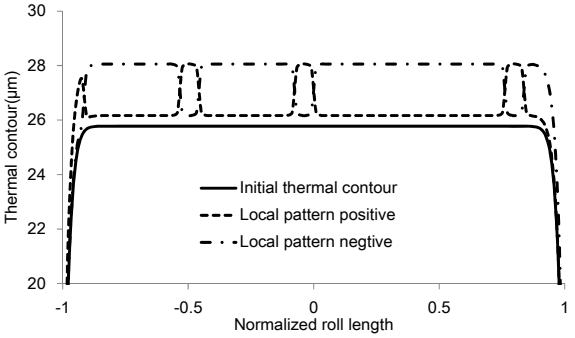

Fig. 7. Thermal contour under local pattern coolant.

Table 3 shows the thermal contour adjustment ranges of each pass.

Table 3. Thermal contour adjustment ranges.

Pass	1	2	3
Cubic pattern positive/ μm	3.74	3.98	3.4
Cubic pattern negative/ μm	-3.74	-3.98	-3.4
Quartic pattern positive/ μm	3.92	4.18	3.56
Quartic pattern negative/ μm	-3.62	-3.86	-3.32
Local pattern positive/ μm	3.78	4.04	3.5
Local pattern negative/ μm	-3.78	-4.02	-3.46

It is apparent that at different passes the subsectional cooling control ability varies, but the positive and negative range are almost the same, indicating that rolling parameters have an effect on the adjustment range but not on the relation between positive and negative range.

5.2. Effect of Rolling Length

Fig. 8 shows the relation between thermal contour adjustment range and rolling length.

The thermal contour adjustment reaches 58 % of its maximum at the first 400 m rolling length, correlating with the change of the work roll surface temperature, indicating that the work roll thermal contour establishes fully at a rather long rolling length.

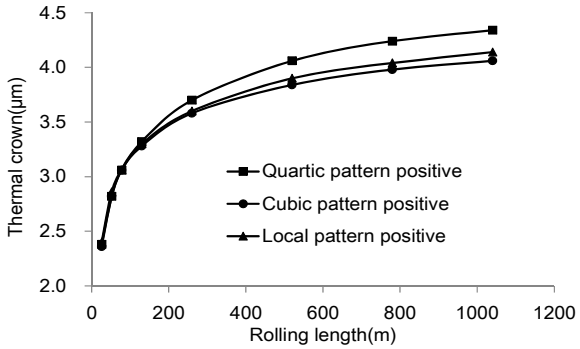

Fig. 8. Relation between thermal contour adjustment range and rolling length.

5.3. Effect of Nozzle Pressure

The thermal contour adjustment range at different nozzle pressure is shown in Fig. 9, having a similar trend with the average heat transfer coefficient. Nozzle pressure is usually between 4~6 bar.

When the control ability of subsectional cooling is insufficient, increasing the nozzle pressure can help.

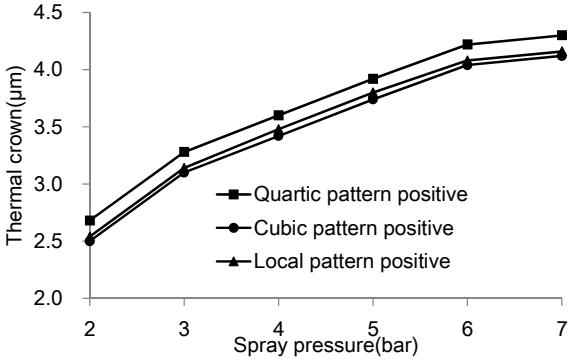

Fig. 9. Thermal contour adjustment range at different nozzle pressure.

5.4. Effect of Rolling Speed

The thermal contour adjustment range reduces by half, when the rolling speed increases from 100 to 300 m/min, as shown in Fig. 10, and from 300 to 600 m/min, the drop gradually decreasing and stabilizing.

Comparing the simulation results of work roll temperature and thermal contour adjustment range, as the roll speed increasing, the promotion of the heat transfer due to the higher work roll surface temperature is overwhelmed by the reduction due to the shorter effective cooling time, so the adjusting range drops.

However, if the rolling speed is too slow, the oil film between strip and roll can break down, and the productivity can't meet the requirement.

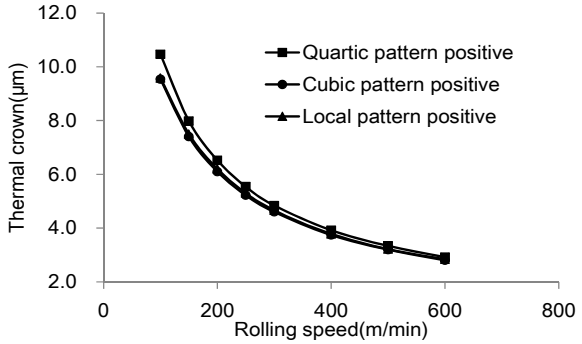

Fig. 10. Thermal contour adjustment range at different rolling speed.

5.5. Effect of Friction Coefficient

Compared to rolling speed, friction coefficient has a relatively small effect on the thermal contour adjustment range, as shown in Fig. 11. The work roll temperature becomes higher as friction coefficient increasing, which promotes the heat transfer of subsectional cooling.

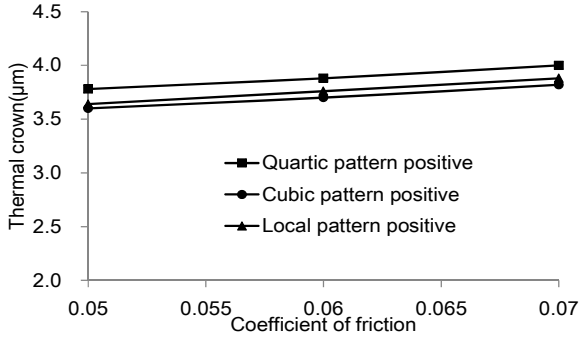

Fig. 11. Thermal contour adjustment range at different coefficient of friction.

6. Conclusions

The simulation results show that the increase of rolled length, working pressure of header and coefficient of friction has positive effect on control ability of subsectional cooling, and the rolling speed is on the contrary. On the beginning of the pass, when work roll surface has not reached the stable temperature, control ability of subsectional cooling is mainly affected by rolled length. The effect of mean coefficient of convective heat transfer and coefficient of friction is linear. When rolling speed is over 500 m/min, control ability of subsectional cooling becomes stable.

Acknowledgements

This work was supported by Beijing Higher Education Young Elite Teacher Project (YETP0413) and Technology Development Plan of Guangxi Province (2013AA01001).

References

[1]. X. Tao, Advanced technologies of shape control in aluminum strip cold rolling industry on the world, *World Nonferrous Metals*, Vol. 28, Issue 6, 2007, pp. 17-20.

[2]. X. D. Zhou, G. D. Wang, Fuzzy control of work roll segments spray cooling system, *Journal of Northeastern University*, Vol. 18, Issue 1, 1997, pp. 77-80.

[3]. A. M. Campos, D. F. García, N. De Abajo, J. A. González, Real time rule based control of the thermal crown of work rolls installed in hot strip mills, *Transactions on Industry Applications*, Vol. 40, Issue 2, 2004, pp. 642-649.

[4]. A. F. M. Arif, O. Khan, A. K. Sheikh, Roll deformation and stress distribution under thermo-mechanical loading in cold rolling, *Journal of Materials Processing Technology*, Vol. 147, Issue 2, 2004, pp. 255-267.

[5]. M. Abbaspour, A. Saboonchi, Work roll thermal expansion control in hot strip mill, *Applied Mathematical Modelling*, Vol. 32, Issue 12, 2008, pp. 2652-2669.

[6]. D. Weiszt, A. Ehrlacher, N. Legrand, Temperature and heat flux fast estimation during rolling process, *International Journal of Thermal Sciences*, Vol. 75, Issue 1, 2014, pp. 1-20.

[7]. J. G. Cao, Y. J. Qin, J. Zhang, Numerical study on parameters of multi-zone cooling for work roll based on unsteady VOF model of Fluent, *Journal of Central South University*, Vol. 42, Issue 12, 2011, pp. 3742-3747.

[8]. J. C. Lian, Rolled strip flatness control theory and the theory, *China Machine Press*, 2013.

[9]. L. J. Xu, Cold rolling mill shape control strip and model selection, *Metallurgical Industry Press*, 2007.

[10]. A. A. Tseng, Thermal modeling of roll and strip interface in rolling processes: part 1-review, *Numerical Heat Transfer*, Vol. 35, Issue 2, 1999, pp. 115-133.

[11]. A. K. Tieu, P. B. Kosasih, A. Godbole, A thermal analysis of strip-rolling in mixed-film lubrication with O/W emulsions, *Tribology International*, Vol. 39, Issue 12, 2006, pp. 1591-1600.

[12]. X. Y. Guo, A. R. He, J. Shao, Modeling and simulation of subsectional cooling system during hot aluminum rolling, *Journal of Mechanical Engineering*, Vol. 49, Issue 4, 2013, pp. 70-74.